

# The lifespan quantitative trait locus gene *Securin* controls hematopoietic progenitor cell function



Andreas Brown,<sup>1</sup> Desiree Schuetz,<sup>1</sup> Yang Han,<sup>2</sup> Deidre Daria,<sup>3</sup>  
Kalpana J. Nattamai,<sup>3</sup> Karina Eiwen,<sup>1</sup> Vadim Sakk,<sup>1</sup> Johannes Pospiech,<sup>1</sup>  
Thomas Saller,<sup>1</sup> Gary van Zant,<sup>4</sup> Wolfgang Wagner<sup>2</sup> and Hartmut Geiger<sup>1,3</sup>

<sup>1</sup>Institute of Molecular Medicine and Stem Cell Aging, Ulm University, Ulm, Germany; <sup>2</sup>Helmholtz-Institute for Biomedical Engineering, Stem Cell Biology and Cellular Engineering, RWTH Aachen University Medical School, Aachen, Germany; <sup>3</sup>Division of Experimental Hematology and Cancer Biology, Cincinnati Children's Hospital Medical Center and University of Cincinnati, Cincinnati, OH, USA and <sup>4</sup>University of Kentucky College of Medicine, UK Medical Center, Lexington, KY, USA

**Haematologica** 2020  
Volume 105(2):317-324

## ABSTRACT

The percentage of murine hematopoietic stem and progenitor cells, which present with a loss of function upon treatment with the genotoxic agent hydroxyurea, is inversely correlated to the mean lifespan of inbred mice, including the long-lived C57BL/6 and short-lived DBA/2 strains. Quantitative trait locus mapping in BXD recombinant inbred strains identified a region spanning 12.5 cM on the proximal part of chromosome 11 linked to both the percentage of dysfunctional hematopoietic stem and progenitor cells as well as regulation of lifespan. By generating and analyzing reciprocal congenic mice for this locus, we demonstrate that this region indeed determines the sensitivity of hematopoietic stem and progenitor cells to hydroxyurea. These cells do not present, as previously anticipated, with differences in cell cycle distribution; neither do they present with changes in the frequency of cells undergoing apoptosis, senescence, replication stalling and re-initiation activity, excluding the possibility that variations in proliferation, replication or viability underlie the distinct response of these cells from the congenic and parental strains. An epigenetic aging clock in blood cells was accelerated in C57BL/6 mice congenic for the DBA/2 version of the locus. We verified pituitary tumor-transforming gene-1 (*Pttg1*)/*Securin* as the quantitative trait gene regulating the differential response of hematopoietic stem and progenitor cells to hydroxyurea treatment and which might therefore be linked to the regulation of lifespan.

## Introduction

We previously reported a correlation between the frequency of hematopoietic stem and progenitor cells (HSPC) from a set of inbred mouse strains with impaired progenitor cell function upon treatment with hydroxyurea (HU) and the mean lifespan of these mice. The set of inbred strains also included C57BL/6 (B6) (low frequency of HSPC dysfunctional in response to HU, long lifespan) and DBA/2 (D2) (high frequency of HSPC dysfunctional in response to HU, short lifespan). In these experiments, the *in vitro* cobblestone area forming cell (CAFC) assay was used to determine the number of functional HSPC before and after treatment with HU. Given that HU kills proliferating cells *via* the induction of DNA strand breaks that arise from stalled replication forks after depletion of the nucleotide pool, this finding was interpreted as a significantly higher percentage of HSPC from D2 *versus* B6 in S-phase, and subsequently that elevated levels of HSPC proliferation could be negatively linked to lifespan.<sup>1-3</sup> Using BXD recombinant inbred (RI) mice, which are genetic chimeras based on B6 and D2, subsequently a quantitative trait locus (QTL) was mapped to chromosome 11 linked to the frequency of HSPC susceptible to HU. Interestingly, the same locus showed also a linkage to the mean lifespan within the BXD RI set of mice, transforming the reported phenotypic correlation into a genetic connection, implying a common underlying gene and thus mechanism for

## Correspondence:

HARTMUT GEIGER  
hartmut.geiger@cchmc.org

Received: November 25, 2018.

Accepted: May 9, 2019.

Pre-published: May 9, 2019.

doi:10.3324/haematol.2018.213009

Check the online version for the most updated information on this article, online supplements, and information on authorship & disclosures: [www.haematologica.org/content/105/2/317](http://www.haematologica.org/content/105/2/317)

©2020 Ferrata Storti Foundation

Material published in *Haematologica* is covered by copyright. All rights are reserved to the Ferrata Storti Foundation. Use of published material is allowed under the following terms and conditions:

<https://creativecommons.org/licenses/by-nc/4.0/legalcode>.  
Copies of published material are allowed for personal or internal use. Sharing published material for non-commercial purposes is subject to the following conditions:  
<https://creativecommons.org/licenses/by-nc/4.0/legalcode>, sect. 3. Reproducing and sharing published material for commercial purposes is not allowed without permission in writing from the publisher.



the regulation of both phenotypes. To verify the linkage, and identify the underlying quantitative trait gene, we generated B6 as well as D2 mice that are reciprocally congenic for this locus on chromosome 11.

## Methods

### Mice

Laboratory C57BL/6J (B6), DBA/2J (D2) and BXD inbred mice were obtained from Janvier Labs (France). All mice were fed acidified water and food *ad libitum*, and housed under pathogen-free conditions at the University of Kentucky, Division of Laboratory Animal Resource, the animal facility at CCHMC. Mouse experiments were performed in compliance with the German Law for Welfare of Laboratory Animals and were approved by the Regierungspräsidium Tübingen or approved by the IACUCs of the University of Kentucky and CCHMC.

### Quantitative trait locus mapping

Linkage analysis and determination of the likelihood ratio statistic values for suggestive linkage were performed as described by using WebQTL (<http://www.genenetwork.org/webqtl/main.py?FormID=submitSingleTrait>), identifying the restrictive chromosome 11 locus, among others, correlating to mean life span and HU sensitivity.<sup>3,6</sup>

### Generation of congenic mice

Congenic animals were generated in five generations by a marker-assisted backcrossing strategy as described<sup>3,5,7-9</sup> (Figure 1C). The particular DBA/2J genomic region was derived from BXD31, one of the BXD recombinant inbred strains used in the quantitative trait locus (QTL) mapping and which phenotypically best demonstrated the decline in HSC in old age and the HU sensitivity.<sup>3</sup>

### Preparation of hematopoietic tissue and cells

For the isolation of total bone marrow (BM), tibiae, femur and hips of mice were isolated and flushed using a syringe and a G21 needle. Mononuclear (low density bone marrow, LDBM) cells were isolated by Histopaque low-density centrifugation (#10831, Sigma). Lineage depletion was performed using the mouse lineage cell depletion Kit (#130-090-858, Miltenyi Biotec) according to their protocol.

### Cobblestone area forming cell assay

Cobblestone area forming cell (CAFC) assay was performed as described.<sup>1</sup> Briefly, 1,000 FBMD-1 cells, a stromal cell line, were seeded in each well of 96-well plates. Plates were incubated at 33°C in 5% CO<sub>2</sub>, and used seven days later for CAFC assay. BM cells were either treated with 200 µg/mL HU or its solvent (PBS) and seeded onto the pre-established stromal layers in six dilutions, serially in 3-fold increments from 333 to up to 81,000 cells/well (12 wells per dilution). At this time, the medium was switched from 5% horse serum and 10% fetal bovine serum to 20% horse serum. Alternatively, mice were treated with HU *in vivo* as indicated following bone marrow isolation and seeding. After seven days, all wells were evaluated for the presence or absence of cobblestone areas and the frequency of the appearance of a colony calculated using L-Cal software (STEMCELL Technologies).

### Analysis of the epigenetic aging signature

Analysis of DNA methylation levels was analyzed at three age-associated CG dinucleotides (CpG) as described previously.<sup>10</sup> Briefly, genomic DNA was isolated from blood samples, bisulfite converted, and DNA methylation was analyzed within the three

genes (*Prima1*, *Hsf4*, *Kcns1*) by pyrosequencing. The DNA methylation results at these sites can be integrated into a multivariable model for epigenetic age predictions in B6 mice, which clearly correlate with the chronological age.<sup>10</sup>

### Statistical analysis

All statistical analyses were performed using Student's *t*-test or two-way Anova, when appropriate with GraphPad Prism 6 software. For Figure 4C, linear and non-linear regression was calculated. The number of biological repeats (n) is indicated in the figure legends. Error bars are Standard Error of Mean (SEM).

## Results

Hematopoietic stem and progenitor cells from BXD RI strains show highly divergent reactions when exposed to HU as judged by their ability to form cobblestones on stromal feeder layers in the CAFC assay after seven days of culture (CAFC day 7 assay).<sup>9</sup> Re-analyzing the initial phenotypic data based on the most recent marker map (New Genotypes 2017 dataset) provided for BXD RI strains, we verified the initially identified locus on chromosome 11 (35-75 Mb) linked (with a suggestive threshold of 10.53/10.88) to both HU susceptibility of HSPC as well as mean lifespan of the analyzed mice (Figure 1A and B and *Online Supplementary Tables S1A* and *B*, and *S3*). We used a marker assisted speed congenic approach to obtain a reciprocal set of mice congenic for the chromosome 11 locus (Figure 1C). These novel mouse lines were named line A (D2 onto B6) and K (B6 onto D2). We performed whole genome SNP mapping of our congenic mouse strains to identify the length of the congenic intervals transferred as well as the overlap between the reciprocal strains. Ultimately, the common region transferred in line A and line K spans an 18.6 Mb (8.3 cM) region on chromosome 11 from rs26900200, 37,929,686 bp to rs3088940, 56,516,067 bp with no other transferred intervals stemming from the donor strains that are identical between the two congenic strains. The SNP analysis further revealed a small set of additional congenic regions in both line A and K animals, though not covering identical regions (Figure 1D, *Online Supplementary Table S2* and *Online Supplementary Figure S1*). This interval contains about 130 protein coding genes (*Online Supplementary Table S3*).

Next, based on the CAFC assay, we tested whether the genotype of the locus conferred in the congenic strains correlated with the magnitude of our phenotype of HSPC susceptible to HU. HU treatment efficiently suppresses BrdU incorporation and thus active S-Phase in freshly isolated Lin-cKit<sup>+</sup> (LK) cells from all strains (*Online Supplementary Figure S2A*). Indeed, HSPC isolated from B6 or line K (B6 onto D2) mice presented with a lower frequency of dysfunctional HSPC in response to short-term *in vivo* as well as to *ex vivo* treatment with HU, while inversely, D2 and line A (D2 onto B6) HSPC were more sensitive to HU (Figure 2A and *Online Supplementary Figure S2B*). These data confirm that the interval on chromosome 11 shared among the congenic strains confers this phenotype and might thus contain a gene regulating the response of HSPC to HU.

Since HU inhibits dNTP synthesis,<sup>11</sup> and a lack of dNTP causes replication fork stalling and thus DNA damage and apoptosis,<sup>12</sup> it is believed that the frequency of cells susceptible to HU treatment is an indirect measurement for

the frequency of cells in the S-phase of the cell division cycle. It has been thus concluded that the underlying mechanism of the distinct susceptibility of HSPC from the inbred strains is due to distinct S-phase frequencies. BM cells with the Lin-cKit<sup>+</sup> surface marker combination (hematopoietic progenitor cells, LK cells) are highly enriched for CAFC day 7 cells (*Online Supplementary Figure S2C*). However, analysis of the frequency of LK cells from the inbred and the congenic strains in different stages of the cell division cycle by *in vivo* BrdU incorporation and flow cytometry, as well as that of hematopoietic stem cells (HSC) and less primitive progenitors (LSK), revealed almost identical patterns and especially almost identical frequencies of cells in S-phase among all the strains tested (Figure 2B). HU susceptibility in HSPC does therefore not correlate with the frequency of HSPC in S-phase, which

excludes differences in cycling frequencies as the underlying mechanism for the phenotype observed, as well as in general HU susceptibility as surrogate for the frequency of cells in S-phase. Consistent with that finding was the fact that HSPC from all groups had similar telomere lengths. Short telomeres can be seen as a surrogate marker for high levels of proliferation (*Online Supplementary Figure S2D*). In addition, the frequency of LK and LSK was very similar in all strains, while D2-derived mice displayed a general higher HSC frequency, as already reported,<sup>1</sup> which is, however, not mirrored in B6/line A mice and thus locus-independent. That finding excludes a difference in the number of these cells as a factor contributing to the phenotype (Figure 2C). Furthermore, the frequencies of HSPC undergoing apoptosis upon *ex vivo* HU treatment and under steady state conditions *in vivo* were at a low level

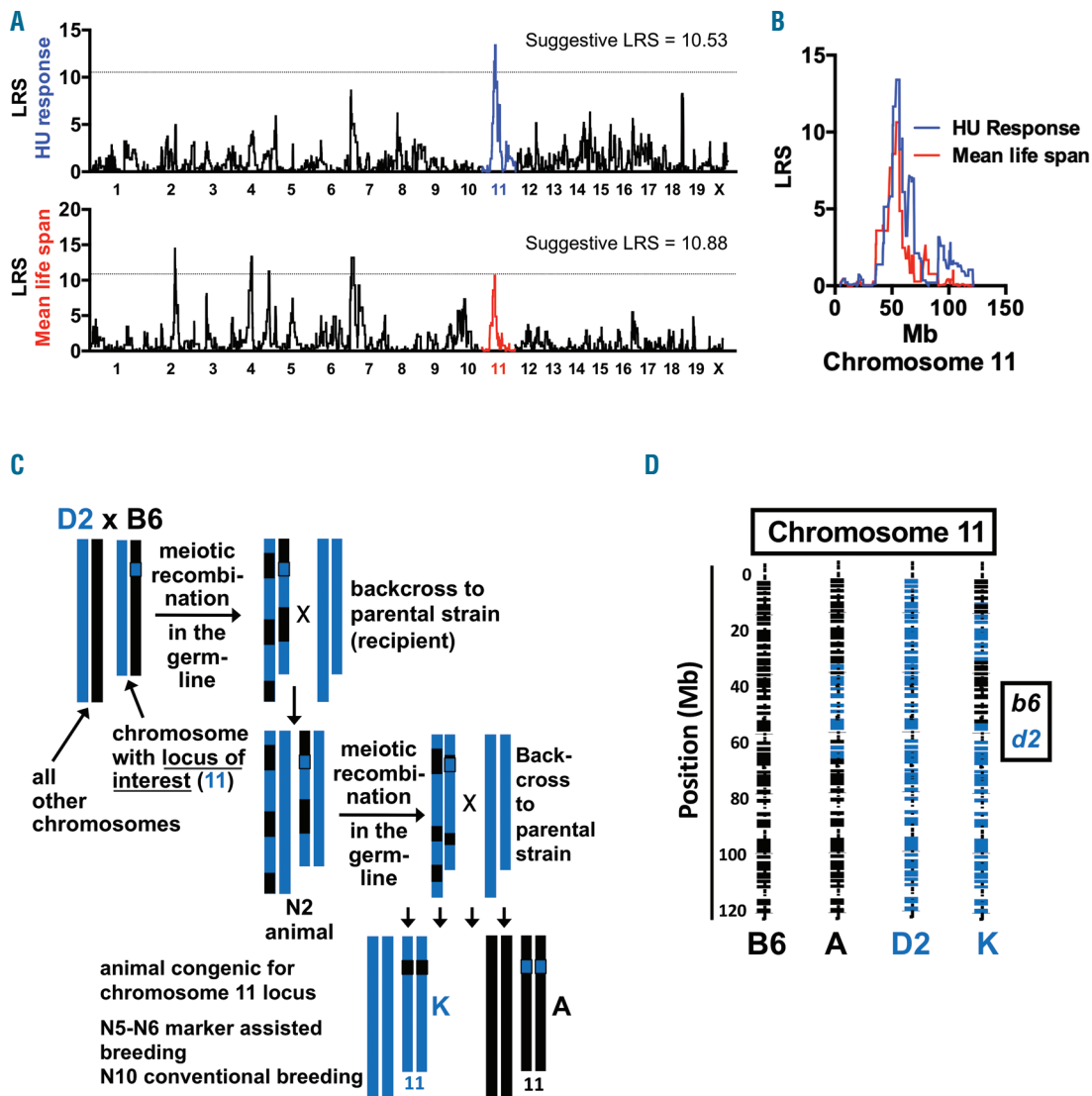


**Figure 1. Quantitative trait locus (QTL) analysis of hydroxyurea (HU) responses and mean life spans of BXD mice and generation of mice congenic for the corresponding chromosome 11 locus.** (A) WebQTL analysis of HU sensitivity rates and mean life spans of hematopoietic stem and progenitor cells (HSPC) isolated from various BXD and parental strains, identifying a proximal part of chromosome 11, among others, involved in this phenotype. Values are in Likelihood Ratio Statistics (LRS). (B) QTL analysis of mean life spans and HU responses of the various BXD strains for chromosome 11. (C) Schematic illustration showing the generation of the congenic mouse strains line A and K. Briefly, after crossing B6 with D2 mice, F1 littermates were backcrossed with the corresponding parental strains (B6/D2). Offspring were backcrossed in four rounds with parental strains reciprocal for the corresponding chromosome 11 specific SNP *D11Mit20* to finally obtain B6 or D2 mice congenic for the proximal locus on chromosome 11 of D2 or B6, respectively. (D) SNP analysis of chromosome 11 from strains B6, D2, A and K.

among these groups, even when regarding S-phase specific apoptosis rates as well senescence in response to HU as indicated by the level of the senescence marker p16 in HSPC (Figure 2D and *Online Supplementary Figure S2E and F*). In addition, whereas HU treatment almost completely blocks BrdU incorporation, LK cells from all strains preserve their ability to re-enter active S-phase in a locus-independent manner 3 and even 16 hours (h) after HU is removed, excluding the possibility that enhanced levels of senescence, apoptosis or difference in re-initiation of replication after stalling are causative for the HU sensitivity phenotype (Figure 2E and *Online Supplementary Figure S2G*). Similarly, LK cells from all strains showed comparable frequencies of  $\gamma$ H2AX foci per cells upon HU treatment and 3 h post HU removal, which also excludes a role of variation in stalling of replication and the subsequent

DNA damage for our phenotype (Figure 2F). In aggregation, these data exclude a likely contribution of differences in cell cycle and replication parameters as well as differential senescence or apoptosis to the highly unequal HU susceptibilities of HSPC in the inbred and congenic strains, while the underlying mechanism still remains to be identified.

A D2-allele at the genetic microsatellite marker *D11Mit174* (Chr.11:42,593,949-42,594,095, which is within the area with the highest level of linkage) correlated in the BXD RI set, as anticipated, with higher HU-susceptibility rates of HSPC and a lower mean life span (Figure 3A). The gene *Pttg1* (*Securin*), which has been reported to inhibit mitotic division,<sup>13,14</sup> is located in very close proximity (+ 800 kb) to *D11Mit174*.<sup>15</sup> In addition, the yeast homolog of *Securin*, *Pds1p*, was reported to be critically

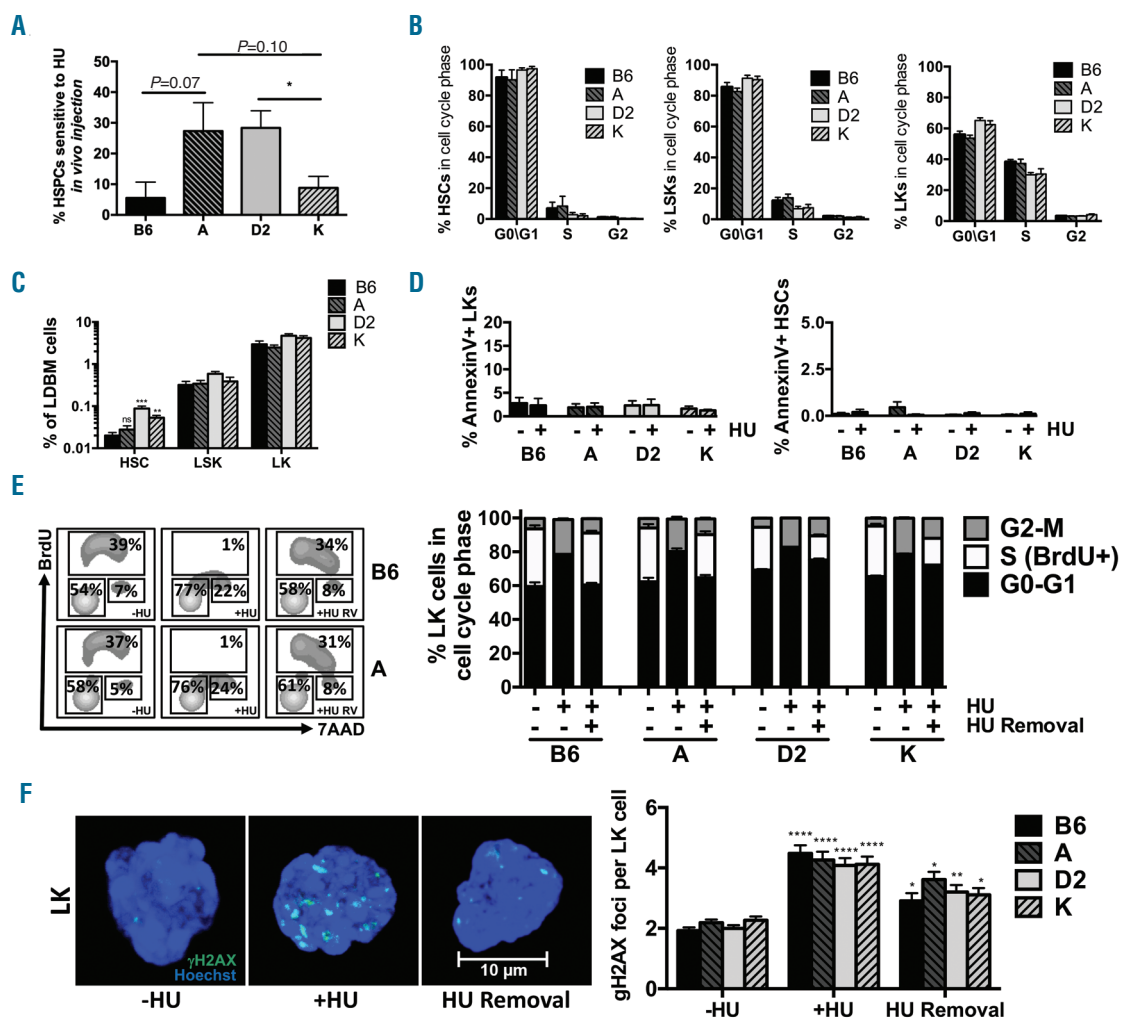


**Figure 2. The chromosome 11 locus controls sensitivity of hematopoietic stem and progenitor cells (HSPC) to hydroxyurea (HU) exposure but not HSPC frequency, cell cycle activity, apoptosis and replication fork stalling.** (A) Mice from all four groups were injected with 10 mg HU/kg body weight or its solvent (PBS) for 1 hour (h) following isolation of bone marrow (BM) cells and processing for the cobblestone area-forming cell (CAFC) assay. Shown is the fraction of HSPC sensitive to HU.  $n=5-12$ . (B) Cell cycle distributions of HSPC (left), Lin-Sca1<sup>+</sup>cKit<sup>+</sup> cells (LSK) (middle) and Lin<sup>+</sup>cKit<sup>+</sup> cells (LK) (right) of bromodeoxyuridine (BrdU)-treated mice.  $n=4$ . (C) Relative low density bone marrow cells (LDBM) frequencies per tibia and femur of Lin<sup>+</sup>cKit<sup>+</sup> cells (LK), Lin-Sca1<sup>+</sup>cKit<sup>+</sup> cells (LSK) and hematopoietic stem cells (HSC) of the four mouse strains.  $n=4$ . (D) (Left) LDBM cells from the four strains were treated with HU or its solvent (PBS) for 1 h. Thereafter, LK cells (left) and HSC (right) were analyzed in terms of apoptosis (AnnexinV).  $n=4$ . (E) LDBM cells were either treated with a control (-HU), HU for 1 h or accordingly following HU removal (RV) by washing twice with medium and an additional resting period of 3 h (+HU RV). Thirty minutes prior to staining, all samples were co-cultured with BrdU. (Left) Representative BrdU/7AAD FACS plots of LK cells from the indicated strains. (Right) Quantification of LK cell cycle distribution.  $n=3$ . (F) LK cells from all four mouse strains were either treated with a control, HU for 1 h or accordingly following HU RV and an additional resting period of 3 h (+HU RV). Thereafter, cells were harvested and stained against  $\gamma$ H2AX. (Left) Representative confocal images. (Right) Quantification of the number of  $\gamma$ H2AX foci per cell.  $n=3$ . Significances are related to the corresponding -HU controls. \* $P<0.05$ ; \*\* $P<0.01$ ; \*\*\* $P<0.001$ ; \*\*\*\* $P<0.0001$ .

involved in the regulation of the intra-S-checkpoint and regulation of the response of yeast to treatment with HU.<sup>16</sup> Previously, a 3-11-fold overexpression of *Pttg1* in various D2 tissues compared to B6 was demonstrated.<sup>17-19</sup> This renders *Pttg1* a prime candidate quantitative trait gene in the interval on chromosome 11. To investigate whether the *Pttg1* mediates the HU response, we analyzed its expression in our experimental mouse strains. We observed a 3-5-fold increase in gene and protein expression in D2 or line A derived HSPC compared to the corresponding cells from B6 or line K mice (Figure 3B and C). A D2-allele of the locus thus confers elevated expression of *Pttg1*. Analyzing *Pttg1*-associated promoter and exon regions in silico revealed a 7 bp insertion downstream of the transcription start (NCBI Reference Sequence: NC\_000077.6) in the D2 genome, potentially positively affecting binding of transcription factors (TF) (Online Supplementary Figure S3A). Since the occurrence of these D2- and A/J-specific 7 bp was previously reported to result in reduced *Pttg1* expression in contrast to what we find in

D2 animals,<sup>20</sup> we further determined the promoter structure of *Pttg1* in more detail by polymerase chain reaction (PCR) of genomic DNA. Surprisingly, the *Pttg1* promoter region was present in two differently sized versions (the two fragments differ in size by approx. 700 bp) in D2 and line A mice (Figure 3D). DNA sequencing revealed that the short version in D2 (D2\_1) was identical to the B6 *Pttg1* promoter, while the longer version (D2\_2) was unique to D2 and included the already described 7 bp insertion in addition to an additional 675 bp region between the transcription and the ORF start, which is not completely annotated in common genome databases at the present time in contrast to the 7 bp insertion (Online Supplementary Figure S3B and C). This could imply a likely gene duplication of *Pttg1* within the congenic locus. We next tested whether the distinct types of promoter regions are causative for the dissimilar *Pttg1* expression patterns. By applying a dual-specific luciferase assay, we observed an almost 3-fold increase in activity of the D2\_2-specific promoter compared to the B6 and the shorter D2\_1 variants, suggesting

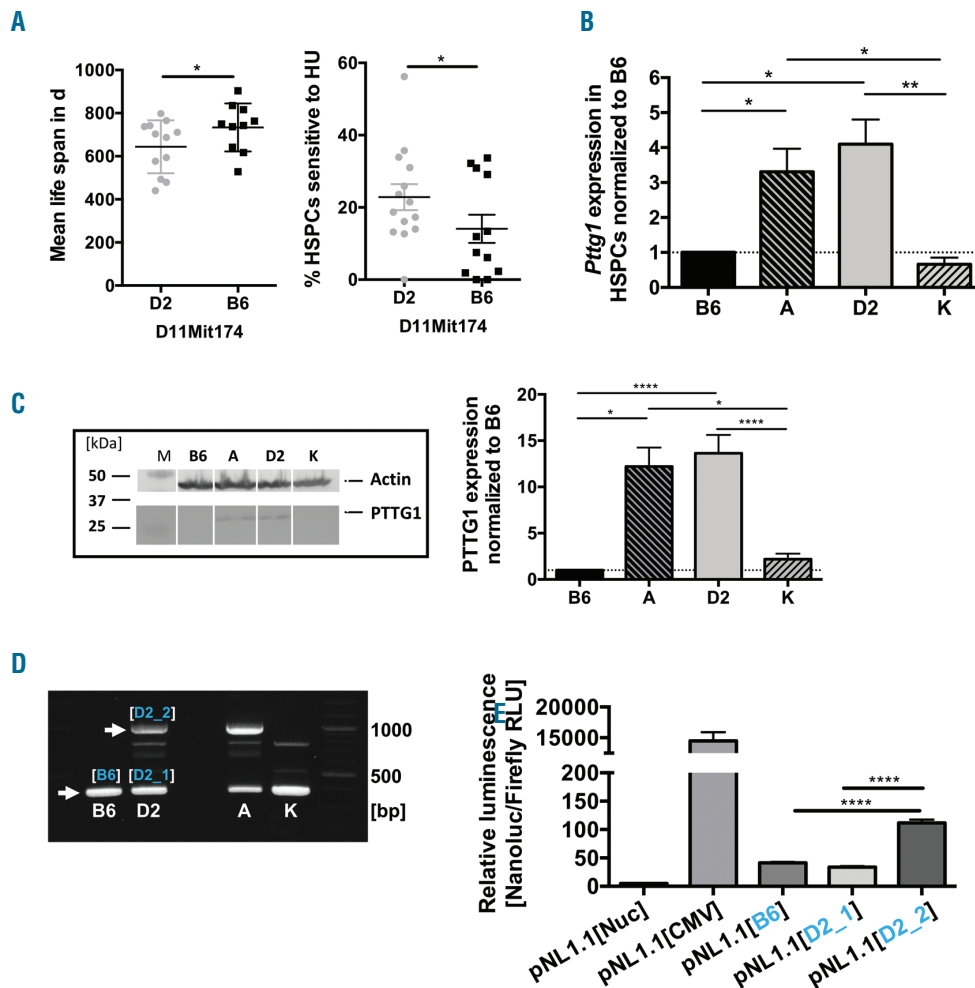


**Figure 3. Chromosome 11 associated *Pttg1* has an altered promoter sequence in D2/A mice leading to enhanced expression.** (A) Mean life span (left) or hydroxyurea (HU) sensitivity rates of hematopoietic stem and progenitor cells (HSPC) (right) of BXD mouse strains relative to the occurrence of the SNP *D11Mit174*. (B) *Pttg1* gene expression in HSPC from the indicated mouse strains. n=3. (C) PTTG1 protein expression in HSPC from the four mouse strains. (Left) Representative western blot images. (Right) Quantification. n=3. (D) Polymerase chain reaction analysis of genomic DNA from lines B6, D2, A and K using the primers 5'NheI-B6/D2\_PTTG1\_pr1 and 3'EcoRV-B6/D2\_PTTG1\_pr2. Major bands corresponding to the different promoters are indicated with arrows. (E) Dual-specific luciferase assay for the indicated promoter constructs, including a negative (pNL1.1[Nuc]) and a positive (pNL1.1[CMV]) control. The corresponding constructs to Figure 3D are highlighted in blue. n=3 (3 rounds with triplicates). \*P<0.05; \*\*P<0.01; \*\*\*\*P<0.0001.

that not the 7 bp insertion but the additional 675 bp region drive elevated levels of *Pttg1* expression in D2 or A cells (Figure 3E). We also identified several exon-specific SNP causing amino acid substitutions in *Pttg1*. Using 3D *in silico* models that predict the protein structure of PTTG1, no obvious difference in the structure was observed between the B6 and D2 variants besides a slight increase in 310 helices, a common secondary structure, which renders an additional contribution of the coding SNP of *Pttg1* to the phenotype less likely (Online Supplementary Figure S4A).

To test whether *Pttg1* is indeed the QTL gene within the described locus, and thus whether the increased HU-sensitivity of HSPC is caused by elevated *Pttg1* levels, we over-

expressed a *Pttg1*-Egfp fusion gene by lentiviral transduction in B6 HSPC. The level of expression of the transgene was within the range of the difference in gene expression between B6 and D2 HSPC and thus in a physiological range (Figure 4A, left panel). Transduced BM cells were transplanted into B6 recipients for their *in vivo* expansion. We sorted GFP<sup>+</sup> BM cells five weeks post transplantation to analyze the susceptibility of HSPC to HU with the CAFC assay. BM cells of the transplanted mice were presented with similar rates of transduction (GFP<sup>+</sup> cells), excluding a potential bias of certain subpopulations upon transduction (Online Supplementary Figure S4B and C). Elevated expression of *Pttg1* in B6 HSPC resulted in a significant increase

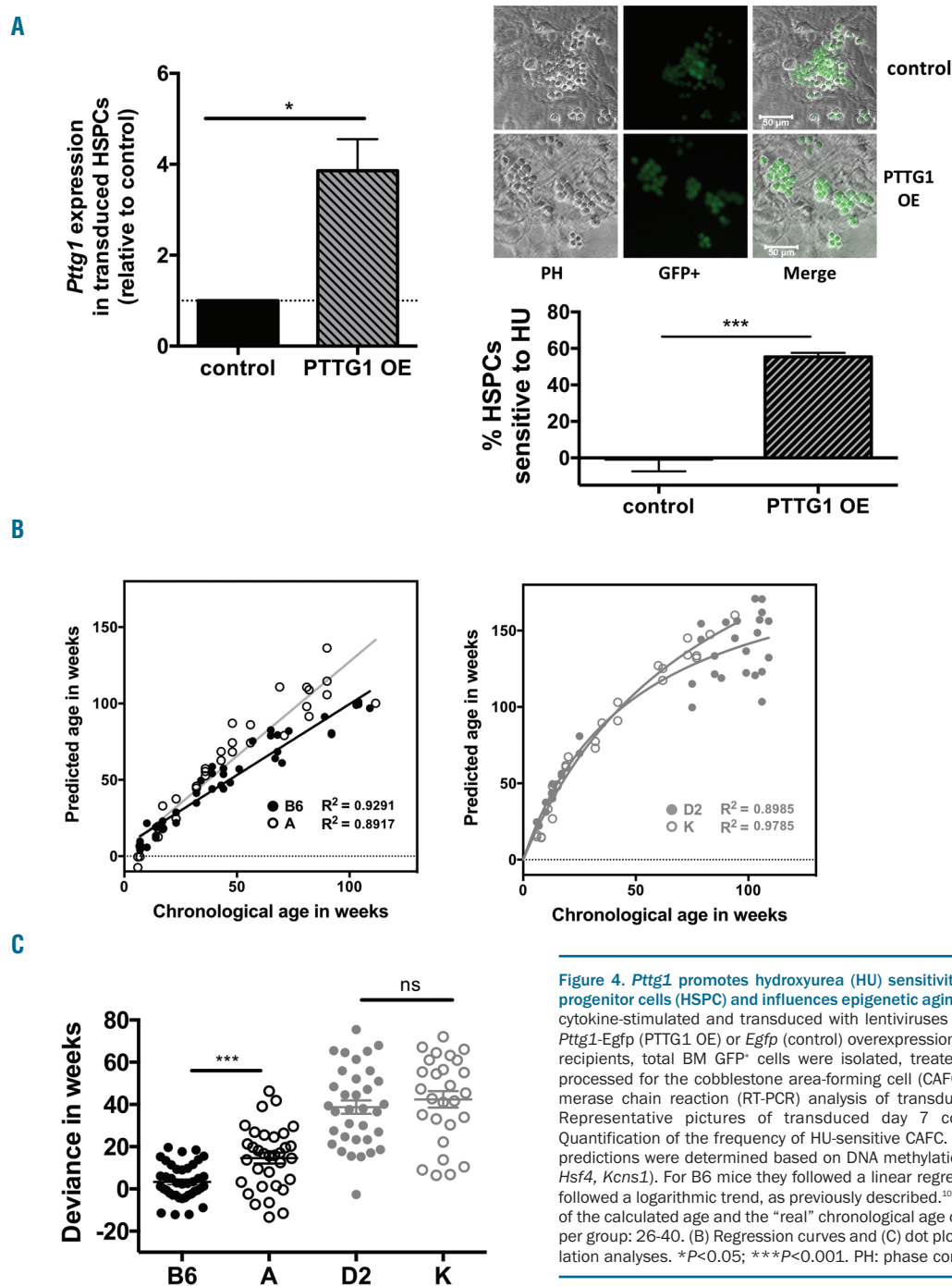


**Figure 4. *Pttg1* promotes hydroxyurea (HU) sensitivity of hematopoietic stem and progenitor cells (HSPC) and influences epigenetic aging.** (A) HSPC from B6 mice were cytokine-stimulated and transduced with lentiviruses mediating stable endogenous *Pttg1*-Egfp (PTTG1 OE) or *Egfp* (control) overexpression. After transplantation into B6 recipients, total BM GFP<sup>+</sup> cells were isolated, treated with HU or its solvent and processed for the cobblestone area-forming cell (CAFC) assay. (Left) Real-time-polymerase chain reaction (RT-PCR) analysis of transduced (GFP<sup>+</sup>) HSPC. (Right top) Representative pictures of transduced day 7 cobblestones. (Right bottom) Quantification of the frequency of HU-sensitive CAFC. n=3. (B and C) Epigenetic age predictions were determined based on DNA methylation at three CpG sites (*Prima1*, *Hsf4*, *Kcns1*). For B6 mice they followed a linear regression curve, whereas for D2 it followed a logarithmic trend, as previously described.<sup>10</sup> The deviance is the difference of the calculated age and the “real” chronological age of the four mouse strains. Mice per group: 26-40. (B) Regression curves and (C) dot plots of the corresponding methylation analyses. \* $P < 0.05$ ; \*\*\* $P < 0.001$ . PH: phase contrast; ns: not significant.

in their susceptibility to HU treatment (Figure 4A, right panel). Similarly, upon downregulation of *Pttg1* in progenitor cells from line A and D2 mice, we observed a trend towards reduced HU sensitivity (Online Supplementary Figure S4D). These data confirm a causative role for distinct levels of expression of *Pttg1* for the susceptibility of HSPC to short-term HU treatment, and thus strongly imply that *Pttg1* is the QTL gene within the QTL locus.

Ultimately, the question remains whether the locus also accounts for a variation in life span. Previously, the methylation status of CpG sites within the genes *Prima1*, *Hsf4*, *Kcns1* was shown to qualify as a reliable predictor of chronological age of B6 mice.<sup>10</sup> This same study also revealed enhanced epigenetic aging of the D2 strain in accordance with its general reduced mean life span, supporting the possibility that the panel might also serve as a marker for the biological age in mice. Applying this B6-trained marker panel to our (congenic) experimental strains, we observed that epigenetic age predictions correlated with chronological age in B6 ( $R^2=0.93$ ) and line A mice ( $R^2=0.89$ ). Notably, epigenetic aging was clearly accelerated in line A mice compared to B6 (Figure 4B and C). We have previously demonstrated that in D2 mice the same epigenetic age predictor significantly accelerated epigenetic age predictions that rather follow a logarithmic regression,<sup>10</sup> which, however, line K did not deviate from (Figure 4B and C). More in depth analyses for line K would warrant the development of an improved age predictor that is adjusted to more control samples of D2, as the initial marker panel was trained on B6. However, the data are consistent with a possible role of the QTL in affecting lifespan at least of line A mice, which will need to be tested in longevity studies of larger cohorts of animals.

## Discussion

Forward genetic approaches in BXD RI strains have been shown to allow for the identification of QTL linked to lifespan and changes in various tissues and cells upon aging.<sup>22,23</sup> We previously reported the likely linkage of a locus on the distal part of murine chromosome 11 to two phenotypes, regulation of lifespan as well the susceptibility of HSPC to short-term treatment with HU. While this finding implies a common mechanism of regulation for the two phenotypes, speculations on the mechanistic connection between these two phenotypes remains difficult without the identification of the gene within the locus regulating at least one of the phenotypes. Here, by generating and analyzing reciprocal strains congenic for the interval on chromosome 11 (B6 onto D2 and D2 onto B6), we verify the initial linkage analysis by demonstrating that this locus indeed controls the susceptibility of HSPC to HU. Other loci than the chromosome 11 locus may at least in part also contribute to the HU response phenotype, as line A and K mice are also congenic for other loci in addition to the locus on chromosome 11 (Online Supplementary Figure S4). The proximal locus on chromosome 11, which spans about 18.6 Mb, is, however, the only region which is identical between both congenic mouse strains, making a substantial contribution of other loci less likely (Online Supplementary Table S2). Unexpectedly, elevated sensitivity of HSPC to HU is not linked to altered cell cycle activity and thus elevated numbers of HSPC in S-phase, nor to apoptosis, senescence or

enhanced replication fork stalling as might be anticipated by previously reported outcomes to HU exposure. The precise mechanism that confers elevated susceptibility thus still remains to be further investigated. Our data strongly support *Pttg1/Securin* to be the QTL gene in that interval, as elevated levels of its expression conferred by the D2 allele result in increased HU susceptibility of HSPC. Recently, *Pttg1* overexpression was reported to restrict BrdU incorporation and cause enhanced levels of senescence and DNA damage in proliferating human fibroblasts,<sup>24</sup> a feature which is not mirrored in HSPC according to our data. Thus, these mechanistic differences illustrate the unique properties of HSPC with respect to cell cycle regulation and DNA damage response, as also demonstrated recently.<sup>25-27</sup> The initial linkage data also imply a role for *Pttg1* in regulating lifespan. The primary role of *Pttg1* is an inhibition of Separase. This cysteine protease opens cohesin rings to allow for transition from metaphase to anaphase.<sup>28</sup> *Pttg1* is thus seen primarily as a target of the anaphase promoting complex (APC/C) to initiate chromosome segregation, although other additional roles have been described in the literature, such as a central role in pituitary tumor formation when overexpressed.<sup>29</sup> Interestingly, the APC/C is directly involved in regulating lifespan in yeast and results in dysregulation of rDNA biology,<sup>30</sup> while likely dominant negative mutations in cohesin genes have been recently identified as novel contributors to the initiation of acute myeloid leukemia through modulation of chromatin accessibility in HSPC and subsequent inhibition of differentiation by recruiting “stemness” transcription factors to the daughter cells upon division. Extended presence of cohesin, in the case of elevated levels of *Pttg1*, might thus contribute to loss of HSPC potential, which would be consistent with our phenotype (Online Supplementary Figure S4B). Hence, the two phenotypes might be mechanistically connected via alterations in the epigenetic landscape rather than changes in chromatid cohesion itself. This interpretation is supported by the finding that age-associated DNA methylation changes are acquired at a different pace in congenic mouse strains. It is thus possible that HU treatment interferes with epigenetic parameters regulated by *Pttg1/Securin*.

## Acknowledgments

We thank the FACS core at Ulm University, especially Ali Gawanbacht-Ramhormose and Sarah Warth for cell sorting and the Central Animal Facility of Ulm University as well as the Comprehensive Mouse and Cancer Core at CCHMC for help with mouse experiments. We are grateful to José Cancelas for providing FBMD-1 stromal feeder cells. We thank Karin Müller from the Internal Medicine III Department for assistance with the GloMax 96 luminometer, Sebastian Iben from the Dermatology Department for helpful advice regarding the promoter studies and all lab members for fruitful discussions.

## Funding

Work in the laboratory of HG is supported by the Deutsche Forschungsgemeinschaft SFB 1074, the RTG 1789, and FOR 2674. AB was supported by a Bausteinprogramm of the Medical Faculty of Ulm University. WW was supported by the Else Kröner-Fresenius-Stiftung (2014\_A193); by the Interdisciplinary Center for Clinical Research within the faculty of Medicine at the RWTH Aachen University (O3-3); by the Deutsche Forschungsgemeinschaft (WA 1706/8-1 and WA1706/11 1).

## References

- De Haan G, Nijhof W, Van Zant G. Mouse strain-dependent changes in frequency and proliferation of hematopoietic stem cells during aging: correlation between lifespan and cycling activity. *Blood*. 1997; 89(5):1543-1550.
- Lopes M, Cotta-Ramusino C, Pellicoli A, et al. The DNA replication checkpoint response stabilizes stalled replication forks. *Nature*. 2001;412(6846):557-561.
- De Haan G, Bystrykh LV, Weersing E, et al. A genetic and genomic analysis identifies a cluster of genes associated with hematopoietic cell turnover. *Blood*. 2002;100(6):2056-2062.
- Geiger H, Rennebeck G, Van Zant G. Regulation of hematopoietic stem cell aging in vivo by a distinct genetic element. *Proc Natl Acad Sci USA*. 2005; 102(14):5102-5107.
- Geiger H, True JM, De haan G, Van Zant G. Age- and stage-specific regulation patterns in the hematopoietic stem cell hierarchy. *Blood*. 2001;98(10):2966-2972.
- Manly KF, Cudmore RH, Meer JM. Map Manager QTX, cross-platform software for genetic mapping. *Mamm Genome*. 2001; 12(12):930-932.
- Van Zant G, Holland BP, Eldridge PW, Chen JJ. Genotype-restricted growth and aging patterns in hematopoietic stem cell populations of allophenic mice. *J Exp Med*. 1990; 171(5):1547-1565.
- Wakeland E, Morel L, Achey K, Yui M, Longmate J. Speed congenics: a classic technique in the fast lane (relatively speaking). *Immunol Today*. 1997;18(10):472-477.
- De Haan G, Van Zant G. Dynamic changes in mouse hematopoietic stem cell numbers during aging. *Blood*. 1999;93(10):3294-3301.
- Han Y, Eipel M, Franzen J, et al. Epigenetic age-predictor for mice based on three CpG sites. *Elife*. 2018;7.
- Young CW, Schochetman G, Karnofsky DA. Hydroxyurea-induced inhibition of deoxyribonucleotide synthesis: studies in intact cells. *Cancer Res*. 1967;27(3):526-534.
- Koç A, Wheeler LJ, Mathews CK, Merrill GF. Hydroxyurea arrests DNA replication by a mechanism that preserves basal dNTP pools. *J Biol Chem*. 2004;279(1):223-230.
- Funabiki H, Kumada K, Yanagida M. Fission yeast Cut1 and Cut2 are essential for sister chromatid separation, concentrate along the metaphase spindle and form large complexes. *EMBO J*. 1996;15(23):6617-6628.
- Funabiki H, Yamano H, Kumada K, Nagao K, Hunt T, Yanagida M. Cut2 proteolysis required for sister-chromatid separation in fission yeast. *Nature*. 1996;381(6581):438-441.
- Hood HM, Metten P, Crabbe JC, Buck KJ. Fine mapping of a sedative-hypnotic drug withdrawal locus on mouse chromosome 11. *Genes Brain Behav*. 2006;5(1):1-10.
- Schollaert KL, Poisson JM, Searle JS, Schwanekamp JA, Tomlinson CR, Sanchez Y. A role for *Saccharomyces cerevisiae* Chk1p in the response to replication blocks. *Mol Biol Cell*. 2004;15(9):4051-4063.
- Bottomly D, Walter NA, Hunter JE, et al. Evaluating gene expression in C57BL/6J and DBA/2J mouse striatum using RNA-Seq and microarrays. *PLoS One*. 2011; 6(3):e17820.
- Geisert EE, Lu L, Freeman-anderson NE, et al. Gene expression in the mouse eye: an online resource for genetics using 103 strains of mice. *Mol Vis*. 2009;15:1730-1763.
- Freeman NE, Templeton JP, Orr WE, Lu L, Williams RW, Geisert EE. Genetic networks in the mouse retina: growth associated protein 43 and phosphatase tensin homolog network. *Mol Vis*. 2011;17:1355-1372.
- Keeley PW, Zhou C, Lu L, Williams RW, Melmed S, Reese BE. Pituitary tumor-transforming gene 1 regulates the patterning of retinal mosaics. *Proc Natl Acad Sci USA*. 2014;111(25):9295-9300.
- Vadnais C, Davoudi S, Afshin M, et al. CUX1 transcription factor is required for optimal ATM/ATR-mediated responses to DNA damage. *Nucleic Acids Res*. 2012; 40(10):4483-4495.
- Lang DH, Gerhard GS, Griffith JW, et al. Quantitative trait loci (QTL) analysis of longevity in C57BL/6J by DBA/2J (BXD) recombinant inbred mice. *Aging Clin Exp Res*. 2010;22(1):8-19.
- Henckaerts E, Langer JC, Snoeck HW. Quantitative genetic variation in the hematopoietic stem cell and progenitor cell compartment and in lifespan are closely linked at multiple loci in BXD recombinant inbred mice. *Blood*. 2004;104(2):374-379.
- Hsu YH, Liao LJ, Yu CH, et al. Overexpression of the pituitary tumor transforming gene induces p53-dependent senescence through activating DNA damage response pathway in normal human fibroblasts. *J Biol Chem*. 2010; 285(29):22630-22638.
- Moehrl BM, Nattamai K, Brown A, et al. Stem Cell-Specific Mechanisms Ensure Genomic Fidelity within HSCs and upon Aging of HSCs. *Cell Rep*. 2015;13(11):2412-2424.
- Brown A, Pospiech J, Eiwien K, et al. The Spindle Assembly Checkpoint Is Required for Hematopoietic Progenitor Cell Engraftment. *Stem Cell Reports*. 2017; 9(5):1359-1368.
- Brown A, Geiger H. Chromosome integrity checkpoints in stem and progenitor cells: transitions upon differentiation, pathogenesis, and aging. *Cell Mol Life Sci*. 2018;75(20):3771-3779.
- Luo S, Tong L. Structural biology of the separase-securin complex with crucial roles in chromosome segregation. *Curr Opin Struct Biol*. 2018;49:114-122.
- Sapochnik M, Nieto LE, Fuertes M, Arzt E. Molecular Mechanisms Underlying Pituitary Pathogenesis. *Biochem Genet*. 2016;54(2):107-119.
- Sun D, Luo M, Jeong M, et al. Epigenomic profiling of young and aged HSCs reveals concerted changes during aging that reinforce self-renewal. *Cell Stem Cell*. 2014; 14(5):673-688.